Published online January 12, 2004

Nucleic Acids Research, 2004, Vol. 32, No. 1 ***211–222***
DOI: 10.1093/nar/gkh177

Modifications of the 3′-UTR stem–loop of infectious bursal disease virus are allowed without influencing replication or virulence

Hein J. Boot* and Sylvia B. E. Pritz-Verschuren

Animal Sciences Group, Wageningen University and Research Centre, Lelystad, The Netherlands

Received October 3, 2003; Revised November 5, 2003; Accepted November 17, 2003

ABSTRACT

Many questions regarding the initiation of replication and translation of the segmented, double-stranded RNA genome of infectious bursal disease virus (IBDV) remain to be solved. Computer analysis shows that the non-polyadenylated extreme 3′-untranslated regions (UTRs) of the coding strand of both genomic segments are able to fold into a single stem–loop structure. To assess the determinants for a functional 3′-UTR, we mutagenized the 3′-UTR stem–loop structure of the B-segment. Rescue of infectious virus from mutagenized cDNA plasmids was impaired in all cases. However, after one passage, the replication kinetics of these viruses were restored. Sequence analysis revealed that additional mutations had been acquired in most of the stem–loop structures, which compensated the introduced ones. A rescued virus with a modified stem–loop structure containing four nucleotide substitutions, but preserving its overall secondary structure, was phenotypically indistinguishable from wild-type virus, both *in vitro* (cell culture) and *in vivo* (chickens, natural host). Sequence analysis showed that the modified stem–loop structure of this virus was fully preserved after four serial passages. Apparently, it is the stem–loop structure and not the primary sequence that is the functional determinant in the 3′-UTRs of IBDV.

INTRODUCTION

Infectious bursal disease virus (IBDV), an avibirnavirus, is the causative agent of the highly contagious disease among chickens known as Gumboro disease, named after the place where it was first discovered (1). IBDV is especially cytopathic to certain B lymphocytes. The highest concentration of these specific B lymphocytes is found in the bursa of Fabricius. In susceptible chickens, damage caused by IBDV can be seen within 2–3 days after exposure to virulent virus. Initially, the bursa of Fabrisius swells (3 days post-exposure) with oedema and haemorrhages and then begins to show atrophy (7–10 days). Destruction of the B lymphocytes by IBDV may result in an incomplete seeding of these cells in secondary lymphoid tissue. As a result of the depletion of B lymphocytes, surviving birds are immunocompromised during the remainder of their lifetime. The disease has spread globally, and commercially raised chickens are vaccinated with live vaccines consisting of attenuated field strains. Variants of the classical wild-type strains that differ either in pathological pattern and antigenic make-up (antigenic variants) or in virulence (very virulent strains) have been isolated [for a review see Van Den Berg (2)].

The birnavirus genome consists of two segments of double-stranded RNA (dsRNA). The largest IBDV dsRNA segment (A-segment, 3260 bp) contains two partly overlapping open reading frames (ORFs), and encodes the minor (VP3) and major (VP2) capsid proteins (see Fig. 1). The smaller genome segment (B-segment, 2827 bp) encodes only one protein, the RNA-dependent RNA polymerase (RDRP, VP1). VP1 has multiple functions, as it is also covalently linked to the 5′ ends of the genomic RNA segments (viral protein genome-linked, VPg) (3,4).

Thus far, only limited data on the initiation of translation and replication of birnaviridae have been published. For example, whether or not the mRNA also contains the same VPg as the genomic RNA is still unknown. The birnavirus mRNAs neither have a 5′-cap structure nor an internal ribosome entry site (IRES) of normal (i.e. >300 nt) length to recruit host cell-encoded initiation factors. Therefore, the VPg at the 5′-untranslated region (UTR) of birnavirus mRNAs is believed to play a functional role in the initiation of translation. Whether the same VPg (the 90 kDa RDRP) is present on the 5′ end of both the plus and minus strands of the double-stranded genomic segments in the viral particle is still unknown. All 3′ termini (positive and negative strand of both the A- and B-segments) of IBDV and IPNV (infectious pancreatic necrosis virus, an aquabirnavirus) end with at least two constitutive cytosines (see Fig. 1). These 3′-UTR cytosines will allow protein-primed initiation of second strand RNA synthesis using VPg-linked guanines (3). The conservation of adjacent cytosines at the 3′ termini of the birnavirus plus-stranded RNA supports the hypothesis that the 5′ termini of the negative-stranded RNA will also have a covalently linked VPg.

The 3′ end of the birnavirus mRNAs differ from cellular mRNAs as no poly(A) tail is present. Poly(A) tails have been shown to protect against 3′–5′exonuclease degradation (5). Furthermore, poly(A) tails enhance the translation efficiency

*To whom correspondence should be addressed. Tel: +31 302744596; Fax +31 302744449; Email: Hein.Boot@RIVM.NL

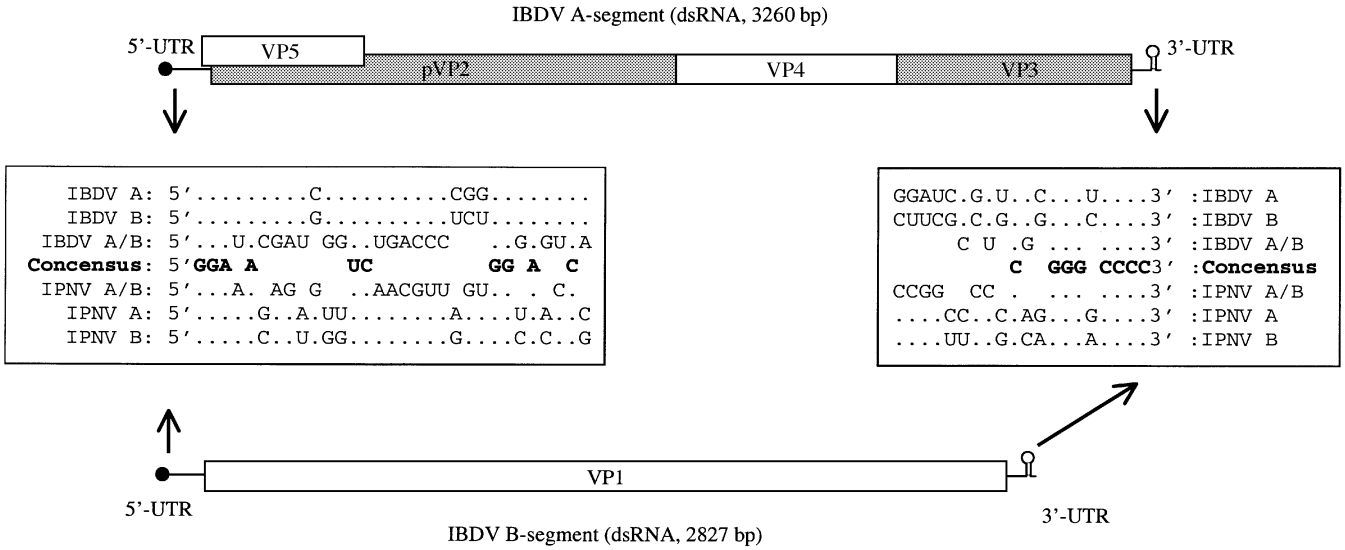

Figure 1. Schematic representation of the segmented dsRNA genome of IBDV. Structural elements such as the VPg (black circle), the 3′-UTR stem–loop structure and open reading frames (boxes) are indicated. The capsid-forming proteins are represented by shaded boxes. Sequence identities in the 5′-UTR (30 nt) and 3′-UTR (20 nt) between the A- and B-segments of both IBDV and IPNV are given. The first three (GGA) and last four nucleotides (CCCC) of each segment are identical. Sequence alignment is based upon the published sequence of IBDV (14) and IPNV (32) with the following accession numbers: AF194428 (IBDV-A), AF194429 (IBDV-B), AF078668 (IPNV-A) and AF078668 (IPNV-B). All these cDNA segments have been used to produce infectious virus (reverse genetics), and therefore contain no functional mutations.

via the interaction with the poly(A)-binding protein (PABP), which circularizes the mRNA by its interaction with eIF4G, the scaffolding component of the pre-initiation complex (6). Competition for initiation of translation between viral and cellular mRNA is an important issue, and different viruses use different strategies to compete with cellular mRNAs for translation initiation factors (7). Just how the non-poly(A) IBDV mRNA resolves the problems of recruiting translation factors without a poly(A) tail is unclear at present.

Secondary structure formation (stem–loop structures) in the 3′-UTR of RNA viruses is often found to play a role in translation efficiency and (initiation) of replication. Secondary structure prediction of the 3′-UTR region of both the A- and B-segment of IBDV showed that single stem–loop structures can be formed by the last 25 nt of the 3′-UTR (see Fig. 2). Such a three-dimensional structure might protect the IBDV mRNAs against exonuclease degradation, but might also enhance the initiation of translation by binding of cellular proteins that promote circularization of the viral mRNA, or assist in initiation of replication by direct or indirect binding of the viral RDRP.

To determine whether mutations introduced in the predicted stem–loop structure are tolerated, and/or lead to compensating or reversion mutations, we changed several nucleotides in the predicted stem–loop structure of the B-segment. Based on the sequence analysis of rescued viruses of mutagenized cDNA, we conclude that the secondary structure, and not the primary structure, is an essential determinant of the 3′-UTR for obtaining viable virus.

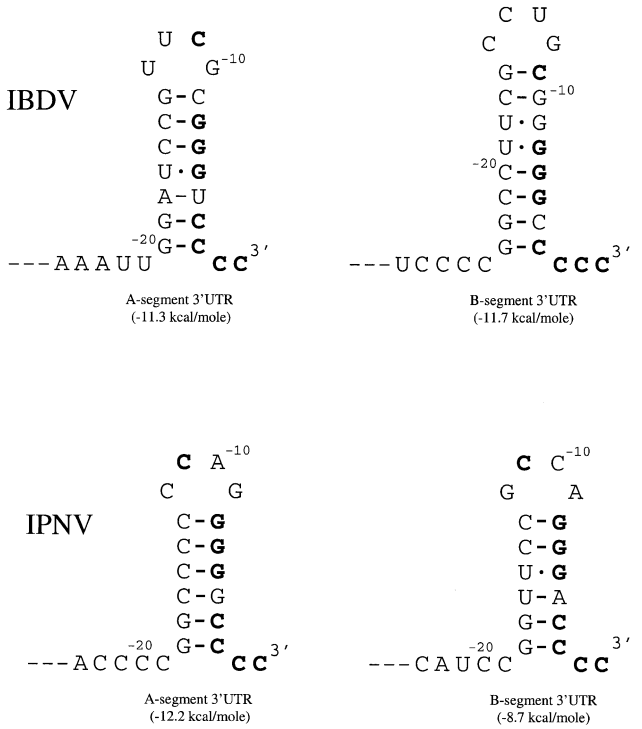

Figure 2. Schematic representation of the predicted (Mfold, version 3.0) stem–loop structure in the extreme 3′-UTRs of the A- and B-segments of IBDV and IPNV. The nucleotides that are conserved over all segments (see also Fig. 1) are given in bold. Energy levels for each stem–loop structure are given in kcal/mol in parentheses.

MATERIALS AND METHODS

Viruses, cells, eggs and antibodies

The classical IBDV isolate CEF94 is a derivative of PV1 (8), which is able to replicate in non-B-lymphoid cells. The D6948 strain is a very virulent field isolate (Poultry Health Service, Doorn, The Netherlands, 1989), which only grows in primary B-lymphoid cells (9). Recombinant fowlpox T7 virus containing the T7 polymerase gene (10) was a kind gift of M.

Skinner (Compton Laboratory, Berks, UK). QM5 cells (11) were maintained by using QT35 medium (Gibco-BRL), supplemented with 5% fetal calf serum (FCS) and 2% antibiotic solution (complete medium) (9). Embryonated SPF eggs (Spafas) obtained from Charles River Laboratories were brooded for 11 days before infection with rIBDV-containing solution (200 µl) using the chorioallantoic membrane route (12). The VP3 monoclonal antibody (mAb) 9.7 was prepared in our laboratory using purified CEF94 as an antigen (13).

Introduction of nucleotide substitutions in the cDNA plasmid of the B-segment

Mutations in the 3′-UTR of the B-segment cDNA plasmid of CEF94 [pHB-34Z (14)] were introduced by using specific oligonucleotides (MB-1–MB-13 and MB-1R2R), which contain the 5′-UTR sequence of the negative B-segment strand, and one or more nucleotide substitutions in comparison with the wild-type CEF94 sequence. A PCR was performed using one mutant oligo together with oligo BC10, pHB-52 as template, and Pwo polymerase (Boehringer Mannheim) as enzyme. The pHB-52 plasmid is a derivative of pHB-34Z that contains an NgoMIV restriction site at nucleotide 2741. These PCR fragments were subsequently purified, digested with NgoMIV and used to replace the corresponding part of plasmid pHB-52 (digested with NgoMIV and SmaI). Cloning was performed using the Rapid DNA-ligation kit of Boerhingher Mannheim (in accordance with the supplier's instructions). Mutant plasmids pMB-1–pMB-13 were recovered after transformation and selection of *Escherichia coli* (DH5α) cells, using the Qiagen Tip-100 purification method according to the supplier's (Qiagen GmbH, Germany) instructions. The presence of the introduced mutations in all mutant B-segment plasmids was confirmed by nucleotide sequence analysis. Secondary structure prediction of the altered 3′-UTR of the coding strand of the B-segment RNA was done using the Mfold program (version 3.0) (15).

Co-transfection of fowlpox T7-infected QM5 cells with the IBDV cDNA plasmids

Purified pMB plasmids were co-transfected with the pHB-36W plasmid into QM5 cells. Plasmid pHB-36W contains the A-segment cDNA of CEF94 preceded by a T7 polymerase promoter, followed by the hepatitis delta virus ribozyme (14). Prior to co-transfection, the QM5 cells were infected for 1 h with fowlpox T7 virus as described before (14). After transfection, the cells were rinsed with phosphate-buffered saline (PBS), covered with complete medium and incubated for 24 h at 37°C (5.0% CO_2). Next, the cells and supernatant were freeze–thawed three times, filtered through a 100 nm pore size filter (Acrodisc, Gelman Sciences) and stored at –20°C. All transfection experiments were carried out at least twice, independently. The amount of infectious rIBDV particles was determined by a $TCID_{50}$ (50% tissue culture infectious dose) assay. Fresh QM5 cells were infected in a 96-well plate with 10-fold dilutions of the filtered transfection lysates and the rIBDV-infected wells were visualized in an immunoperoxidase monolayer assay (IPMA) using an IBDV-specific mAb directed against VP3. The staining of IBDV-infected cells using specific antibodies was necessary as some of the rescue mutants (i.e. vMB-10) resulted only in individually infected cells and did not yield plaques or CPE after 48 h of incubation.

Serial passages of rescued rIBDV

To determine the stability of the introduced mutations, we serially cultivated the mutant rCEF94 on QM5 cells four times. The mutant rCEF94, which appeared to have a non-wild-type B-segment 3′-UTR sequence in the fourth passage, was serially cultivated until the tenth passage. During each passage, the freeze–thawed lysate of a culture was filtered through a 200 nm pore size filter (Acrodisc, Gelman Sciences), and 10% of the volume was used to re-infect a fresh culture of QM5 cells.

Sequence determination of the 3′-UTR B-segment of rIBDV

To determine the 3′ termini of the plus strands of the B-segments of rCEF94-MB-1–MB-9 of either the fouth or tenth passage on QM5 cells, or from bursa-derived virus, we purified genomic RNA by differential centrifugation and proteinase K treatment as described before (14). Genomic dsRNA was dissolved in 10 µl of poly(A) buffer [50 mM Tris–HCl pH 7.9, 10 mM $MgCl_2$, 5 mM $MnCl_2$, 250 mM NaCl, 1 mM dithiothreitol (DTT), 50 µg/ml bovine serum albumin (BSA), 0.04 U of Rnasin (Promega), in diethylpyrocarbonate (DEPC)-treated water] with 0.25 mM ATP and 1 U of poly(A) polymerase (Pharmacia). After incubation at 37°C for 30 min, the enzyme was denatured by incubation at 75°C for 10 min. The polyadenylated dsRNA was precipitated by ethanol/NaAc, after which the dsRNA was dissolved in 25 µl of DEPC-treated water. To obtain single-stranded copy DNA (cDNA), 2 µl of AmpliTaq buffer II (10×, Perkin-Elmer), 2 µl of $MgCl_2$ (25 mM, Perkin-Elmer), 2 µl of DTT (0.1 M, Gibco-BRL), 1 µl of dNTPs (10 mM each) and 2 µl of UAPdT primer (Promega, 2 pmol/µl) were added to 10 µl of purified polyadenylated RNA. After incubation at 70°C for 2 min, this mixture was immediately transferred onto ice. The dsRNA–primer mixture was subsequently incubated at 52°C for 2 min, after which 1 µl of reverse transcriptase (Superscript II, Gibco-BRL), or no reverse transcriptase (negative control), was added and incubation was continued for 50 min at 52°C. The reverse transcription reaction was terminated by incubation at 75°C for 10 min. The genomic dsRNA and the RNA of the RNA–DNA hybrid were destroyed by the addition of 0.5 µl of RNase A (20 mg/ml, Calbiochem) and 0.5 µl of RNase H (1.2 U/µl, Pharmacia) and incubation at 37°C for 20 min. We used a nested PCR to amplify the single-stranded cDNA. For the first PCR, we used the primers UAP (5′-GGCCACGCGTCGACTAG-3′) and BC9 (5′-GCTCTAGAACTTGTGGAAACAAGCGA-3′), and for the nested PCR we used the primers UAPN (5′-CCACGCGTCGACTAGTAC-3′) and BC10 (5′-GCTCTAGATCAAGAACCCACAGACCG-3′). The mixture for the first PCR was as follows: 2 µl of cDNA, 10 pmol of each specific primer, 2.5 mM $MgCl_2$, 1× AmpliTaq buffer II (Perkin-Elmer), 50 µM of each dNTP and 1 U of AmpliTaq polymerase (Perkin-Elmer), in a total volume of 50 µl. After incubation at 94°C for 1 min, the amplification was performed in 30 cycles through the different temperature levels: 94°C for 15 s, 52°C for 15 s, and 72°C for 60 s, followed by 3 min at 72°C. For the nested PCR, 16 µl of the first PCR amplification

was separated in an agarose gel (1.5%) and the specific product (372 bp) was partly isolated with a needle and mixed with a 50 µl complete nested PCR mixture. The conditions of the nested PCR were the same as in the first PCR with the following adaptations: a hybridization temperature of 54°C and 3.5 mM $MgCl_2$. The resulting nested PCR product (309 bp) was gel purified and sequence analysis was directly performed on the PCR products.

Growth curves of rIBDV of the fourth passage

To compare the replication ability of the mutant rCEF94 viruses, we obtained single-step growth curves of all mutant B-segment 3′-UTR viruses of the fourth passage. QM5 cells were grown overnight (16 h) in a 60 mm cell culture dish and, after removing the medium, 1 ml of complete medium containing rIBDV (log_{10} $TCID_{50}$ between 6 and 7) was used to cover the cells. After 1 h, the supernatant was removed, the cells were rinsed four times with 8 ml of PBS, and then 5 ml of complete medium was added (t = 1 h). Samples (0.5 ml) were taken from the supernatant at different intervals (1, 5, 10, 15, 25 and 50 h post-infection) and stored at –20°C. The viral titre of each sample was determined in a $TCID_{50}$ assay (see above).

Virulence of rescued IBDV in SPF chickens

Rescued IBDV containing the A-segment of the very virulent IBDV strain D6948 (pDA-60) was first propagated on embryonated eggs by inoculating supernatant of a transfection experiment into 11-day-old embryonated eggs via the chorioallantoic membrane route (12). After 7 days of incubation, the embryos (dead or alive) were recovered. The bodies of the recovered embryos were homogenized in a Sorval Omni-mixer (three times 10 s, max. speed), clarified by centrifugation (6000 *g*, 15 min), and then stored in aliquots at –70°C. The virus titre (50% embryo lethal dose, ELD_{50}) in these samples was determined using 11-day-old embryonated eggs. Four groups of chickens (7 days old) were housed separately in isolators and each chick received 50 ELD_{50} rIBDV in PBS, or only PBS (negative control group) orally. At 7, 14 and 21 days post-infection, five animals were randomly removed and a blood sample was taken before euthanasia. The virus-neutralizing titres in the serum samples were determined as described before (13). Bursa and body weights were determined of all chicks following euthanasia. Samples from the bursa of Fabricius taken at necropsy were fixed in 10% neutral-buffered formalin, dehydrated, embedded in paraffin wax, sectioned and stained with haematoxylin–eosin (H&E). The histopathological bursal lesion score (HBLS) was determined by microscopic analysis of the bursa using the classification: 0 = absence of damage; 1 = necrosis of isolated follicles; 2 = moderate general depletion of lymphocytes or severe depletion limited to a few follicles; 3 = severe depletion of lymphocytes in >50% of follicles; 4 = remains of follicular contours showing a few lymphocytes with hyperplasia of related tissues, cysts, thickened and folded epithelium; 5 = loss of the entire follicular structure with associated fibroblasts.

RESULTS

The 3′-terminal ends of the IBDV mRNAs do not contain a polyadenylated tail, but are predicted to fold into a small stem–loop structure comprising nucleotides –20 to –2 in the case of the A-segment, and –23 to –3 in the case of the B-segment (Fig. 2). To study the function of this stem–loop structure, and to analyse the influence of an altered stem–loop structure on viral viability and replication efficiency, we mutated several of the nucleotides involved in the formation of the stem–loop structure of the B-segment. The desired mutations were introduced during PCR amplification of only a small part of the 3′ part of the B-segment cDNA sequence. This mutated 3′ region was then transferred to the full-length B-segment plasmid clone of CEF89 (pHB-52), and verified by sequence analysis. The mutant B-segment cDNA plasmids were co-transfected with the A-segment cDNA plasmid of

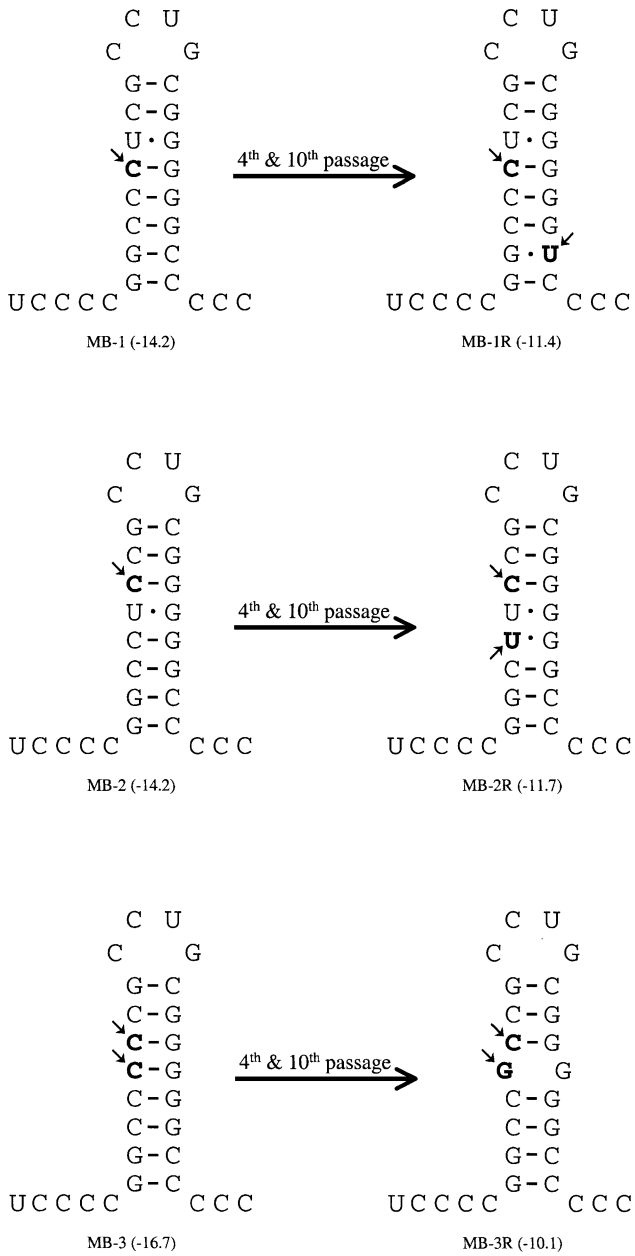

Figure 3. Introduced point mutations in MB-1, -2 and -3, and observed point mutations in the fourth and tenth serial cultivation in comparison with the wild-type sequence, are indicated in bold and with arrows (MB-1R, -2R and -3R, see also legend to Fig. 2).

Table 1. Influence on rescue efficiency by mutations in the B-segment 3′-UTR stem–loop structure

Mutation	Co-transfected cDNA plasmids B-segment	A-segment	Rescue[a]	TCID50[b]
Negative control		pHB-36W	0/8	–
Positive control	pHB-52	pHB-36W	8/8	4.9 (0.6)
$U^{-19}\rightarrow C$	pMB-1	pHB-36W	2/2	3.6 (0.1)
$U^{-18}\rightarrow C$	pMB-2	pHB-36W	2/2	2.5 (0.7)
$U^{-18}U^{-19}\rightarrow CC$	pMB-3	pHB-36W	2/2	2,2 (0.2)
$G^{-16}\rightarrow C$	pMB-4	pHB-36W	2/2	0.3 (0.2)
$G^{-16}C^{-17}\rightarrow CG$	pMB-5	pHB-36W	2/2	0.6 (0.3)
$G^{-10}C^{-11}\rightarrow CG$ and $G^{-16}C^{-17}\rightarrow CG$	pMB-6	pHB-36W	2/2	1.8 (0.4)
$G^{-6}\rightarrow C$	pMB-7	pHB-36W	2/2	1.5 (0.1)
$C^{-5}G^{-6}\rightarrow GC$	pMB-8	pHB-36W	1/2	0.2 (0.2)
$C^{-5}G^{-6}\rightarrow GC$ and $C^{-21}G^{-22}\rightarrow GC$	pMB-9	pHB-36W	2/2	1.1 (0.5)
$C^{-24}\rightarrow G$	pMB-10	pHB-36W	5/6	0.6 (0.3)
$C^{-3}\rightarrow G$ and $C^{-24}\rightarrow G$	pMB-11	pHB-36W	0/2	–
$C^{-24}C^{-25}\rightarrow GG$	pMB-12	pHB-36W	0/2	–
$C^{-24}C^{-25}C^{-26}\rightarrow GGG$	pMB-13	pHB-36W	0/2	–
$C^{-5}\rightarrow U$ and $U^{-18}U^{-19}C^{-20}\rightarrow CCU$	pMB-1R2R	pHB-36W	3/3	4.5 (0.3)

[a]Number of times that infectious virus was obtained after transfection/number of transfection experiments.
[b]Amount of infectious particles at 24 h post-transfection is given as log10 of 50% tissue culture infectious dose ($TCID_{50}$), and the SD is given in parentheses.

CEF89 (pHB-36W) into QM5 cells, which had been infected with recombinant fowlpox virus expressing T7 polymerase prior to transfection. The presence and phenotype of rescued virus was subsequently determined either *in vitro* (cell culture) or *in vivo* [embryonated eggs and specific pathogen-free (SPF) chickens].

Stabilizing mutations in the middle of the B-segment stem–loop structure

Both the A- and B-segment have one (A-segment) or two (B-segment) U–G base pairs in the middle of the stem–loop structure (Fig. 2). Although U–G base pairs are not destabilizing, they do not contribute to the stability of the stem–loop structure. To determine whether a U–G base pair is an essential part of the stem–loop structure, we mutated the lower U–G (pMB-1), the upper U–G (pMB-2) or both the U–G (pMB-3) base pairs of the B-segment stem–loop, by exchanging the uracil for a cytosine (Fig. 3). All the plasmids were co-transfected in duplicate with the A-segment plasmid (pHB-36W) into QM5 cells, and the viral titre was determined at 24 h post-transfection. We were able to easily rescue infectious IBDV from these mutated B-segment plasmids, although the rescue efficiency was ~10-fold (pMB-1) or 100-fold (pMB-2 and -3) lower in comparison with the wild-type B-segment stem–loop (Table 1). The rescued viruses were subsequently serially cultivated three times, and a single-step growth curve for each of them was performed (data not shown). No difference was found in the replication behaviour of these three viruses in comparison with the wild-type CEF94, indicating that the introduced mutations might have already been lost during the four serial passages. Despite the equal growth characteristics, it appeared from sequence analysis of the fourth passage of vMB-1 and -2 that the introduced mutations were still present, and that additional mutations had been acquired (Fig. 3). When one U–G base pair (vMB-1 and vMB-2) was replaced with one C–G base pair, a change of another C–G base pair into a U–G base pair in the stem–loop was found to be present. In the case of vMB-3, where both U–G base pairs were removed, no new U–G base pairs, but a C to G mutation had been acquired, disrupting the middle part of the stem structure (Fig. 3). To evaluate whether the readily acquired mutations were stable during prolonged cultivation, we continued the serial cultivation for an additional six times (p10). No additional mutations in the B-segment of the 3′-UTR were found in p10 in comparison with p4 (Table 2).

Mutations affecting the upper part of the stem structure

The upper part of the B-segment stem–loop is formed by two G–C base pairs (Fig. 2). To investigate the importance of this region, we introduced mutations to disrupt one (pMB-4) or both (pMB-5) of these base pairs. We also made a mutant in which these two G–C base pairs were inverted (pMB-6) (Fig. 4). Rescue of the mutants in which the upper G–C base pair was disrupted (vMB-4) was severely reduced (10 000-fold) and we only obtained infectious virus in one out of the two transfections (Table 1). The mutant in which both G–C base pairs had been disrupted (vMB-5) was also reduced by the same order of magnitude, while the inverted double G–C mutant (vMB-6) was rescued about 1000 times less efficiently. After four serial passages, again no difference was observed between the rescued mutants and the wild-type virus in a single-step growth curve (data not shown). Sequence analysis showed that the introduced mutations in vMB-4 and vMB-6 were still present, but that one additional mutation in either the predicted stem [vMB-4 (p4)] or loop [vMB-6 (p4)] region had been acquired (Fig. 4). No additional mutations were found upon prolonged serial cultivation (p10, Table 2). In vMB-5, the introduced mutations were both reverted, but there was also an additional mutation ($U^{-19}\rightarrow G$) in the stem region [vMB-5 (p4)]. Furthermore, we found a mixed base (a major C and a minor U) at position –5 in the lower part of the stem structure of vMB-5 (4p), indicating a mixed population. Upon prolonged cultivation of vMB-5, we found that the acquired guanine at position –19 was changed into a cytosine ($G^{-19}\rightarrow C$), leading to the formation of a new C^{-19}–G^{-8} base pair

Table 2. Nucleotide sequences of the B-segment cDNA plasmids, and the resulting sequence of the fourth and tenth serial passage of the corresponding rescued IBDV

Name	cDNA plasmid derived sequence[a]	Energy[b]	Sequence in virus of the 4th passage[c]	No. of repeats[d]	Energy[b]	Sequence in virus of the 10th passage[c]	Energy[b]
rCEF94	UCCCCGGCCUUCGCCUGCGGGGGCCCCC	-11.7	UCCCCGGCCUUCGCCUGCGGGGGCCCCC	2*	-11.7	UCCCCGGCCUUCGCCUGCGGGGGCCCCC	-11.7
vMB-1	---------C----------	-14.2	---------C----------U----	4*	-11.4	---------C----------U----	-11.4
			---------C----------U--	1*	-14.6	ND	
vMB-2	----------C----------	-14.2	--------U-C----------		-11.7	--------U-C----------	-11.7
vMB-	----------CC----------	-16.7	----------GC----------		-10.1	----------GC----------	-10.1
vMB-4	----------C----------	-10.4	----------A-C------U--------		-11.5	----------A-C------U--------	-11.5
			----------C------U--------		-7.8		
vMB-5	----------GC----------	-9.2	---------G-**----------U----		-6.1	---------C-**----------U----	-11.4
			---------G-**----------		-8.0	---------C-**----------	-14.2
						---------G-**----------U----	-6.1
						---------G-**----------	-8.0
vMB-6	----------GC----GC----------	-13.3	----------GC---AGC----------		-13.3	----------GC---AGC----------	-13.3
vMB-7	----------C-----	-8.5	----------*-----	5*	-11.7	ND	
vMB-8	----------CG----	-7.8	----------**----		-11.7	ND	
vMB-9	------CG----------CG----	-11.3	------CG-C----------UG----		-11.7	------CA----------UG----	-9.2
			------CG----------UG----		-8.6	------CG----------UG----	-8.6
						------CA-C----------UG----	-12.3
						------CG-C----------UG----	-11.7
vMB-10	----G----------	-14.6	----UA----------		-8.7	----UA----------	-8.7
vMB-11	----G----------G--	-12.3	NV			NV	
vMB-12	---GG----------	-16.7	NV			NV	
vMB-1	--GGG----------	-19.6	NV			NV	
vMB-1R2R	--------UCC----------U----	-11.4	--------UCC----------U----		-11.4	ND	

[a]The given sequences represent nucleotide 2799–2827 of the positive strand of the B-segment of IBDV as found for wild-type virus (CEF94, GenBank accession No. AF194429). The nucleotides identical to wild-type sequence are represented by dashes in the mutant viruses, while mutations that are encoded by the generated mutant cDNA plasmids are given in single letters.

[b]The energy value resulting from the Mfold secondary structure prediction of the sequence in the preceding column is given (in kcal/mol).

[c]Sequences as found in the fourth and tenth passage after rescue using the mutant B-segment cDNA plasmids. Mutations that differ according to the corresponding cDNA sequences are given in bold. Reversions to the wild-type sequences are indicated by asterisks. NV, not viable; ND, not done.

[d]Number of repeats gives the number of independent co-transfection experiments that have been performed with the mutant cDNA plasmid to yield the given sequence in the fourth passage (see Discussion).

(Fig. 4), and that cytosine and uracil were still present at position –5, only now uracil took precedence over cytosine.

Mutations affecting the lower part of the stem structure

To investigate the fidelity of mutations in the lower part of the stem structure, we introduced the same set of mutations as we did in the upper part of the stem [i.e. a single G–C base pair disruption (pMB-7), a double G–C base pair disruption (pMB-8) or the inversion of a double G–C base pair (pMB-9)] (Fig. 5). The rescue efficiencies of the single G–C disruption mutant (vMB-7) and of the double G–C inversion mutant (vMB-9) were both ~1000-fold reduced compared with a wild-type stem–loop structure (Table 1). Rescue of the double G–C mutant (vMB-8) was far more severely reduced (>10 000), and we obtained infectious virus in only one out of the two co-transfections with a very low titre (three infectious particles per ml, Table 1). Again, single-step growth curves did not reveal any difference between the rescued viruses of the fourth serial cultivation, compared with the wild-type virus, suggesting that these mutant viruses had acquired additional mutations. Sequence analysis after four serial passages revealed that in both the single G–C and double disruption [vMB-7 and -8 (p4)], the introduced mutations were lost (reversion into wild-type stem–loop). However, the inverted double G–C mutant [vMB-9 (p4)] appeared to have retained three of the four introduced mutations, while the introduced C^{-6} was replaced by a uracil (Fig. 5). Furthermore, a mixed base was present at position –19, while in the majority the original uracil had been replaced by a cytosine. Serial passages of vMB-9 up to p10 resulted in a more complex situation, as two mixed bases were observed at positions –19 and –21, indicating that evolution and selection of quasispecies had not yet reached equilibrium after 10 passages.

Elongation of the stem structure

The B-segment 3′-UTR stem–loop is flanked on both sides by adjacent cytosines (see Fig. 2). In an earlier study, we demonstrated the importance of at least two non-base pairing cytosines at the 3′-UTR of the IBDV A-segment for efficient rescue, and that these cytosines are restored during replication if artificially removed prior to transfection (14). By introducing mutations adjacent to the stem structure, the predicted length and stability of the stem–loop structure will change, but the availability of non-base-paired 3′-UTR cytosines will also be influenced (Fig. 6). Rescue of virus was successful in four of the four co-transfection experiments when C^{-24} adjacent to the stem–loop was changed into a guanine (pMB-10), although the rescue efficiency was severely reduced (~10 000 less than wild type, Table 1). In contrast to all other viable rescued mutants described in this study, we failed to cultivate this particular rescued virus, even after prolonged cultivation of the transfection supernatants. Re-transformation

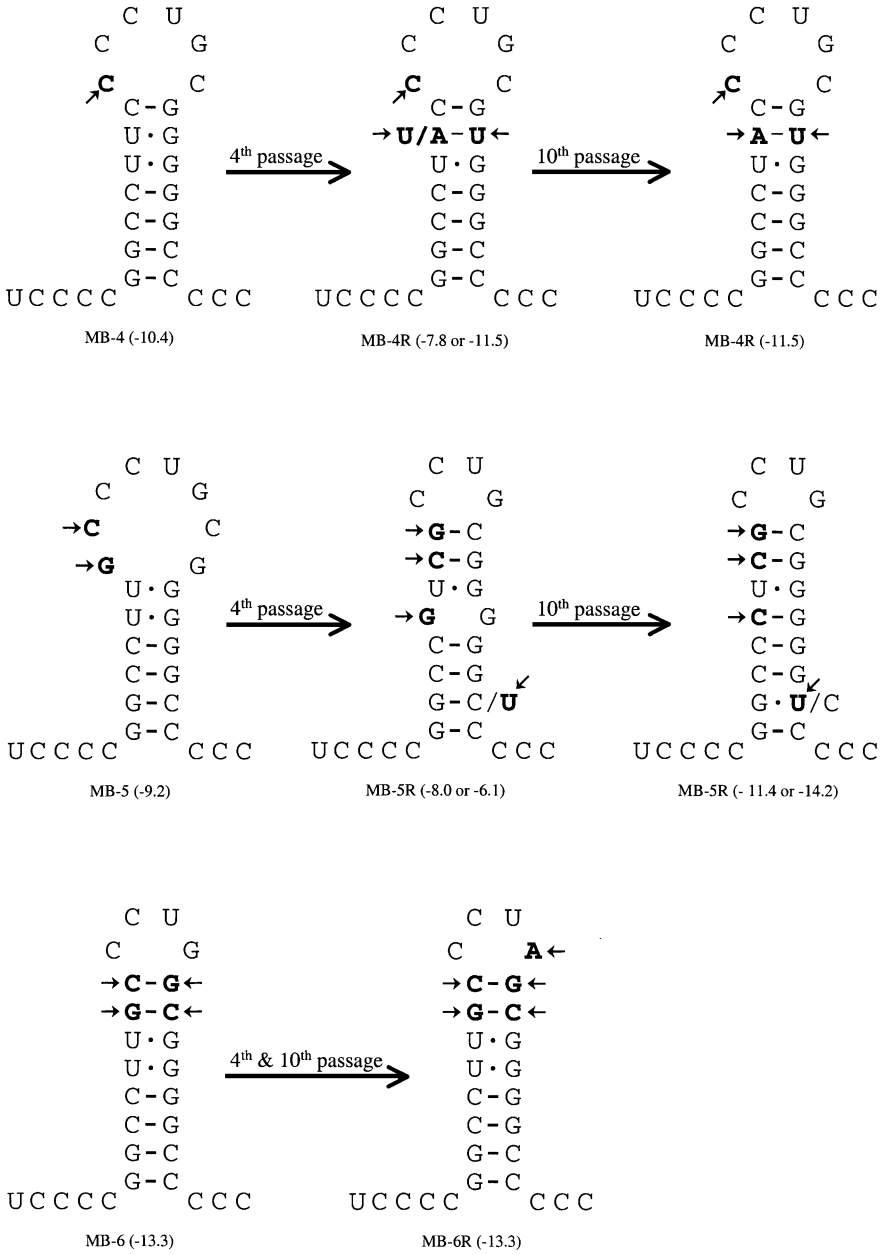

Figure 4. Introduced point mutations in MB-4, -5 and -6, and observed point mutations in the fourth and tenth serial cultivation in comparison with the wild-type sequence, are indicated in bold and with arrows (MB-4R, -5R and -6R, see also legend to Fig. 2). Two nucleotides were present at one position in the case of MB-5R. The predominant nucleotide in each viral culture is given in bold.

(in duplicate) of pMB-10 again yielded viable virus in one case, and after prolonged cultivation CPE appeared. Serial cultivation (p4) of this particular viable mutant yielded virus with replication kinetics equal to wild type (data not shown). Sequence analysis revealed that the introduced G at position –24 had reverted into a U, and that an adjacent mutation was present (G^{-23} was changed into a A) (Fig. 6). No additional changes in the stem–loop region sequence were found after prolonged cultivation (p10). When both cytosines adjacent to the stem structure had changed into guanines (pMB-11), we were unable to rescue viable virus. The same inviability was found when two or three cytosines 5′-adjacent to the stem–loop had been changed into guanines (pMB-12 and -13, Fig. 6). The inviability of vMB-11–vMB-13 could be due to the stabilizing effect of the additional base pairs, but could also be due to the lack of free cytosines, because the free cytosines at the 3′ end are essential for viability (14).

A modified stem–loop structure

Based on the reversion mutations, we assumed that the composition, secondary structure and stability (predicted energy value) were of far greater importance than the primary sequence of the stem–loop structure. To obtain proof for this assumption, we designed a stem–loop structure on the basis of

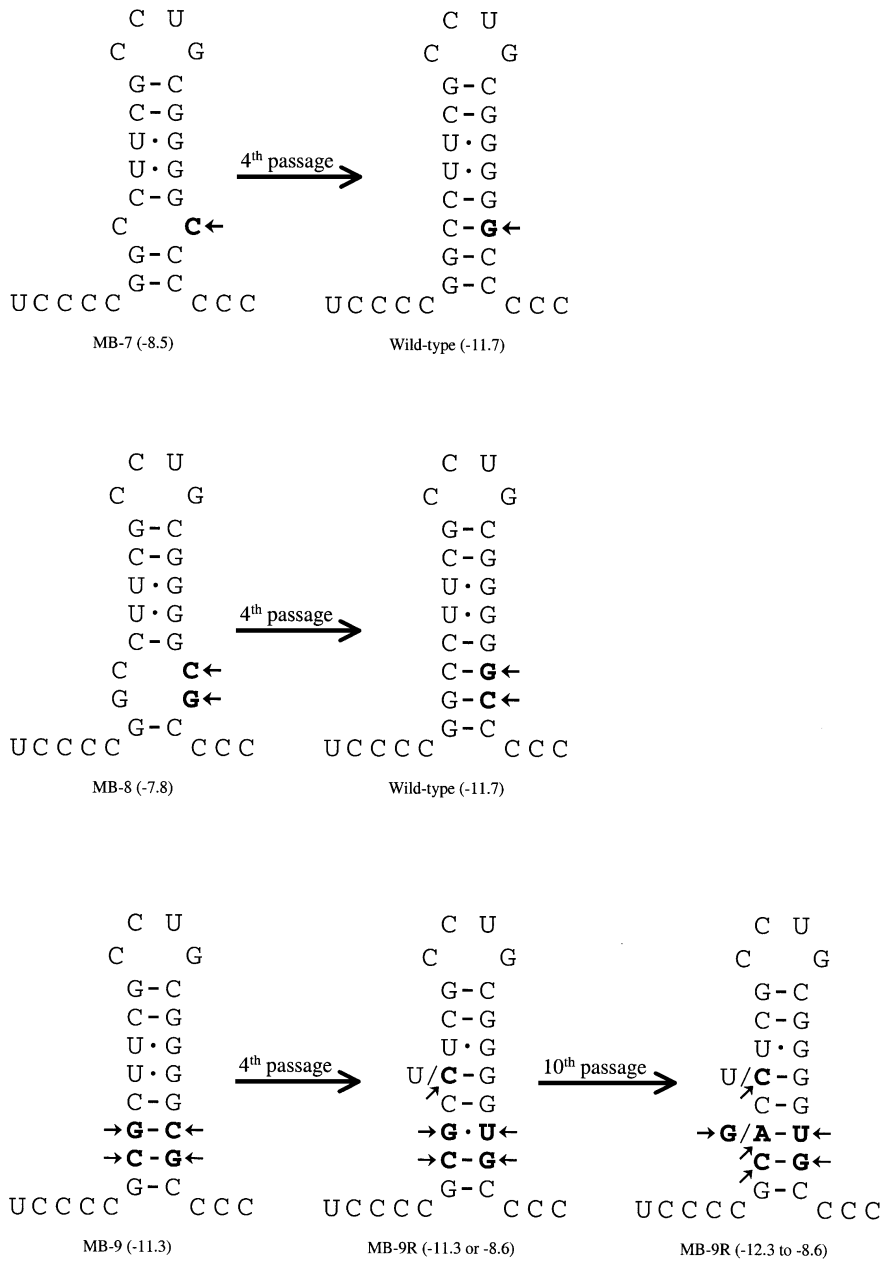

Figure 5. Introduced point mutations in MB-7, -8 and -9, and observed point mutations in the fourth and tenth serial cultivation in comparison with the wild-type sequence, are indicated in bold and with arrows (MB-7R, -8R and -9R, see also legend to Fig. 2). MB-9 showed two different nucleotides at position –19 in the fourth passage, while an even more complex pattern was found in the tenth passage. Predominant nucleotides are given in bold in the case of mixed nucleotides at one position.

the sequences we found in p4 culture of vMB-1 and -2. The pMB-1R2R stem–loop contains four mutations, yielding a stem–loop structure in which four of the six internal base pairs of the stem–loop have been altered, while preserving the nucleotide composition, predicted secondary structure, stability and loop sequence (Fig. 7). Rescue of this virus was equally efficient as rescue of the wild-type virus (Table 1), indicating that this artificial stem–loop structure could replace the wild-type stem–loop structure without loss of function. Sequence analysis after the fourth serial passage indeed showed that this artificial stem–loop structure was completely preserved, and a single-step growth curve of the vMB-1R2R (p4) showed the same replication kinetics as wild-type virus (data not shown).

Very virulent IBDV with a modified B-segment 3′-UTR stem–loop structure

All the above-described stem–loop mutations have been introduced into the genome of the cell culture-adapted isolate CEF94 (14). The specific mutations for growth on cell culture

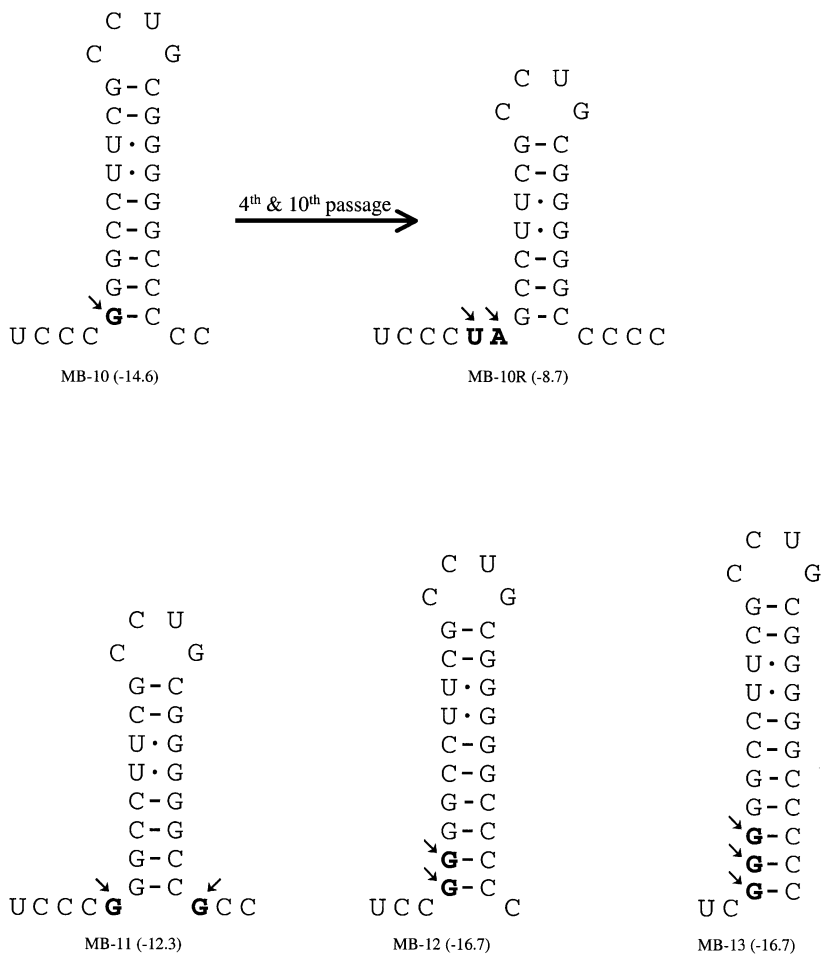

Figure 6. Introduced point mutations in MB-10 -11, -12 and -13, and observed point mutations in the fouth and tenth serial cultivation in comparison with the wild-type sequence, are indicated in bold and with arrows (MB-10, see also legend to Fig. 2). No virus could be rescued after co-transfection of the A-segment with the mutagenized B-segments of MB-11, -12 and -13.

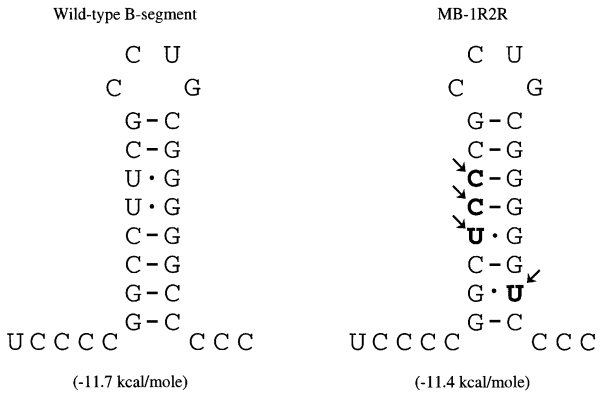

Figure 7. The introduced point mutations (indicated in bold and with arrows, see also legend to Fig. 2) of MB-1R2R are based on the acquired mutations in vMB-1R and -2R. Serial cultivation (fouth and tenth passage) of the vMB-1R2R did not result in any additional mutations or reversions.

are located in the VP2 region of the polyprotein, which is encoded by the A-segment. As a result of these adaptive mutations, the cell culture-adapted isolates are no longer virulent for young chickens, so no data on (loss of) virulence due to introduced stem–loop mutations can be obtained using this genomic background. To analyse the influence of the modified stem–loop structure on the virulence of very virulent IBDV, we rescued a segment-reassorted virus, in which the A-segment (pDA-60) of a wild-type, very virulent D6948 strain is combined with the wild-type (pHB-52) or the modified stem–loop-containing B-segment of CEF94 (pMB-1R2R). Plasmids were co-transfected into QM5 cells, which support the initial replication (9). After filtration, the lysate of the transfected cells was inoculated into embryonated eggs. After egg amplification and titration, SFP chickens at the age of 7 days (37 chickens per group) were orally infected with 50 ELD_{50}. At 7, 14 and 21 days post-infection, five randomly selected birds of each group were removed and virus-neutralizing titres, bursa body weight ratios and the damage to the bursa of Fabricius were determined. No difference was found between the bursal damage (Table 3) or antibody induction (data not shown) of the virus containing the modified stem–loop structure (srIBDV-1R2R) and its unmodified counterpart (srIBDV-DACB). Sequence determination of virus recovered from two bursas of chicks sacrificed at

Table 3. Post-mortem data of SPF chickens infected with wild-type and mutant IBDV

Virus	Bursa/body weight ratio[a] × 1000			HBLS[b]		
	7 d.p.i.	14 d.p.i.	21 d.p.i.	7 d.p.i.	14 d..p.i	21 d.p.i.
Mock	3.9 (1.5)	6.7 (2.1)	6.2 (1.4)	0.0 (0.0)	0.0 (0.0)	0.0 (0.0)
D6948	1.0 (0.3)	1.1 (0.2)	0.9 (0.2)	5.0 (0.0)	4.8 (0.4)	4.6 (0.5)
srD6948-DACB	1.5 (1.0)	1.0 (0.2)	0.9 (0.2)	5.0 (0.0)	5,0 (0,0)	4,4 (0,5)
srD6948-1R2R	1.7 (0.4)	1.2 (0.3)	1.1 (0.2)	5.0 (0.0)	4.8 (0.5)	4.2 (0.4)

[a]For each chicken, the ratio between the weight of the bursa of Fabricius and body was determined. All given data are based on five chickens, at the given days post-infection (d.p.i.). SD is given in parentheses.
[b]Histopathological bursa lesion score (HBLS) was performed on a 0 (healthy) to 5 (completely damaged) scale, see Materials and Methods. All given data are based on five chickens, SD is given in parentheses.

72 h post-infection revealed that the introduced mutations in srIBDV-1R2R had been fully retained.

DISCUSSION

Birnaviruses differ in their genome replication from all other known RNA viruses in that the RDRP (VP1) is also present as a VPg molecule at the 5′ end of both genomic dsRNA segments. Very limited data have been published about the different steps of the replication strategy of the birnavirus genome [for review see Dobos (16)]. The mRNA lacks a 5′ cap structure and only possesses a small 5′-UTR (96–130 nt), which prohibits the formation of an extensive secondary and tertiary structure found to act as an IRES in other RNA viruses (e.g. picorna- and flavivirus) lacking a 5′ cap structure.

Factors in the 3′-UTR as well as in the 5′-UTR play a role in efficient initiation of translation. The IBDV mRNAs are non-polyadenylated, which poses more questions about the recruitment of cellular translation initiation factors in competition with the capped mRNAs of the host cell. A small stem–loop structure, predicted to be present at the extreme 3′ end of both the A- and B-segment of IBDV, seems to play a role in replication and/or translation. Deletion of part of the stem–loop structure in the full length of cDNA results in a reduced rescue efficiency of infectious virus. Furthermore, sequence analysis showed that once rescued, wild-type-like replication kinetics are accompanied by a restored stem–loop structure (14). To obtain further insight into the role of the 3′-UTR stem–loop structures in the translation and/or replication strategies used by birnaviruses, we have, in this study, modified the predicted stem–loop structure of the full-length B-segment cDNA of IBDV, and analysed the sequence in the 3′-UTR stem–loop region of rescued virus after serial cultivation.

Rescue of infectious virus from all mutagenized cDNA plasmids, in which the predicted stem–loop structure was either stabilizing or destabilizing, was impaired or sometimes impossible. However, once infectious virus was obtained, it replicated at a rate indistinguishable from wild-type virus. This suggests that either the introduced mutations were readily lost (reversion) during the first rounds of replication, or that second-site mutations had been acquired, which compensated the introduced mutations. Sequence analysis of rescued virus after the fourth or tenth passage revealed that both events had occurred (see Table 2 for overview). The second-site mutations found in the viable mutants were all present in the stem–loop structure, strongly supporting the formation of this stem–loop in the natural course of infection, and a functional role for this secondary structure in the viral life cycle. Although we cannot exclude that second-site mutations are present in the remainder of the part of the B-segment (or even the A-segment) in some of the mutants, this seems to be unlikely. First, no mutations were observed in the region upstream of the predicted stem–loop structure (~200 nt, encompassing the entire 3′-UTR), which was sequenced in all serially cultivated mutants. Secondly, the mutant virus (MB-1R2R), in which the reversion mutations of vMB-1 and vMB-2 had been combined, yielded rescue titres equalling those found for the rescue of wild-type virus (Table 1), indicating that no functional mutations were present in the remainder of the genome of vMB-1 and vMB-2, to compensate the altered B-stem–loop structure of those rescued viruses. Thirdly, all acquired mutations or reversions (except for vMB-10) appeared before or during the first passage, as full CPE was already present in the first passage at 48 h after infection. The early appearance of the mutations favours single-site mutations, as there is only very limited time for evolution of the more complex double-site mutations.

The limited number of mutations introduced thus far does not allow us to draw conclusions as to whether specific nucleotides in the stem–loop structure are dispensable or not. We found a high proportion of the reversions and second-site mutations to be the result of transversion (12*) and a low proportion attributable to transitions (8*). This reflects the apparent strong constraints on nucleotide composition for this small stem–loop structure. However, it seems that not the primary structure (nucleotide sequence), but rather the secondary structure (stem–loop) is the functional determinant of the 3′-terminal sequence. By combining the observed reversions and second-site mutations of this and an earlier study (14), we draw the following conclusions: (i) mutations decreasing or increasing the predicted stability of the stem–loop structure result in second-site mutations (or reversion), which compensate this deviation; (ii) mutants with an enlarged stem structure (=higher stability) have a dramatic influence on the rescue efficiency, or yield non-viable virus; (iii) introduced mutants and deletions in the 3′ part of the stem structure are all reverted, indicating that the 5′ part of the stem structure is used as template for the 3′ part; and (iv) the exact conservation of the primary sequence of the B-segment loop structure is not essential, as we observed in the fourth and tenth passage of vMB-6, a stable maintained transition ($G^{-12}\rightarrow A$).

An introduced mutation can be compensated in many different ways, and still fulfil the general rules given above. To see whether different introduced mutations always result in the same reversion or second-site mutation, we additionally co-transfected pMB-1 (which results in a second-site mutation) and pMB-7 (which results in reversion) four times each with the A-segment cDNA plasmid. The nucleotide sequence of the fourth passage of these rescued viruses was determined in the 3′ stem–loop region of the B-segment (Table 2). In the case of the second-site mutation observed in vMB-1R (see Fig. 3), we found the same reversion four out of five times. The deviating reversion appeared to have acquired an additional cytosine transition near the 3′ stem part ($C^{-3}\rightarrow U$), which does not contribute to a decrease in the predicted stability of the stem–loop structure. The observed reversion of vMB-7 to wild-type sequence in the fourth passages was also found in the four additional rescued vMB-7 viruses.

Essential stem–loop structures at the extreme 3′-UTR are frequently found in plus-strand viruses [e.g. Picorna- (17), Corona- (18), Flavi (19) and Lentiviridae (20)]. These stem–loop structures are often found to play a role in genome replication (19,21,22) and genome packaging (23). Moreover, it has also been described that 3′-UTR stem–loop structures play a role in protection against 3′–5′exonucleases (24) and in interactions between the 5′- and 3′-UTRs (25). We expect that the predicted 3′-UTR stem–loop in the plus strand of IBDV genomic segments disappears during second-strand synthesis, and will be absent in the dsRNA genomic RNA due to complementarity between plus and minus strands. The absence in the genomic dsRNA would exclude a role for the stem–loop structure in packaging of the genomic dsRNA like that of the LA virus (26). We recently showed that VP3, the structural protein located at the internal face of the capsid, interacts with the double-stranded genomic RNA (27), suggesting that the 3′-UTR stem–loop of the plus strand is indeed dispensable for packaging. We have not yet determined whether either viral- or host-encoded proteins can bind to the IBDV 3′-UTR stem–loop structure. In analogy with systems described for other viruses, we expect, however, that either host proteins (18) or viral proteins (23) indeed can bind this stem–loop structure.

Recruiting the host translation machinery is an important step in viral infection, and the level between viral and host mRNA translation can be influenced in many different ways (7). One efficient way of influencing the ratio between viral and host mRNA translation, applied by Picornaviridae, is by the inactivation of a protein (eIF4G) that is essential for host mRNA initiation of translation, but which is dispensable for viral mRNA initiation of translation (28). *In vitro* IBDV experiments showed that the level of host protein synthesis is not specifically inhibited by an IBDV infection (M.G.J.Tacken and H.J.Boot, submitted), suggesting that IBDV has other means of promoting viral mRNA translation. One commonly known way to enhance translation is the re-use of ribosomes by shuttling them between the 3′- and 5′-UTR of the mRNA. This shuttling is normally seen in host cell mRNAs mediated by interaction of proteins binding to the 3′ poly(A) tail and cap-dependent translation initiation factors (5). Rotavirus, which just like IBDV also has a segmented double-stranded mRNA genome that lack poly(A) tails, has been shown to use the shuttling of ribosome to enhance the viral mRNA translation over the host mRNA translation. By recruiting a host protein involved in translation initiation (eIF4G), the host protein synthesis is decreased, while the viral RNA translation is increased (29). As host shut-off is not found upon IBDV infection, a similar interference with host mRNA translation seems to be absent in IBDV. It has been shown that a direct base pairing between a 5′-UTR of a cellular mRNA and the 18S rRNA can direct initiation of translation of a homeodomain mRNA (30). Although it has been suggested that a similar mechanism might direct translation initiation in birnaviruses (31), we only find little complementarity (4 nt) between the consensus sequence of the 5′-UTRs of IBDV and chicken 18S rRNA, making a direct base pair interaction unlikely. Whether the IBDV 3′-UTR stem–loop structure is able to bind directly or indirectly to one or more host proteins involved in enhancing the translation efficiency remains to be established.

ACKNOWLEDGEMENTS

The assistance of Stephanie Vastenhouw, Daniela Dam and Jos Dekker in preparation of stem–loop mutants and virus rescue is greatly appreciated. We also thank Norbert Stockhofe, Arjan Hoekman and Dirk van Roozelaar for the animal experiment analysis, and Ben Peeters, Arno Gielkens and Paul Steverink for their enthusiastic support during the course of the experiments. Part of this research was funded by Lohmann Animal Health (Cuxhaven, Germany).

REFERENCES

1. Cosgrove,A.S. (1962) An apparently new disease of chickens: avian nephrosis. *Avian Dis.*, **6**, 385–389.
2. Van Den Berg,T.P. (2000) Acute infectious bursal disease virus in poultry: a review. *Avian Pathol.*, **29**, 175–194.
3. Dobos,P. (1993) *In vitro* guanylylation of infectious pancreatic necrosis virus polypeptide VP1. *Virology*, **193**, 403–413.
4. Calvert,J.G., Nagy,E., Soler,M. and Dobos,P. (1991) Characterization of the VPg–dsRNA linkage of infectious pancreatic necrosis virus. *J. Gen. Virol.*, **72**, 2563–2567.
5. Jackson,R.J. and Standart,N. (1990) Do the poly(A) tail and 3′ untranslated region control mRNA translation? *Cell*, **62**, 15–24.
6. Gallie,D.R. (1998) A tale of two termini: a functional interaction between the termini of an mRNA is a prerequisite for efficient translation initiation. *Gene*, **216**, 1–11.
7. Gale,M.,Jr, Tan,S.L. and Katze,M.G. (2000) Translational control of viral gene expression in eukaryotes. *Microbiol. Mol. Biol. Rev.*, **64**, 239–280.
8. Petek,M., D'Aprile,P.N. and Cancellotti,F. (1973) Biological and physico-chemical properties of the infectious bursal disease virus (IBDV). *Avian Pathol.*, **2**, 135–152.
9. Boot,H.J., ter Huurne,A.A., Hoekman,A.J., Peeters,B.P. and Gielkens,A.L. (2000) Rescue of very virulent and mosaic infectious bursal disease virus from cloned cDNA: VP2 is not the sole determinant of the very virulent phenotype. *J. Virol.*, **74**, 6701–6711.
10. Britton,P., Green,P., Kottier,S., Mawditt,K.L., Penzes,Z., Cavanagh,D. and Skinner,M.A. (1996) Expression of bacteriophage T7 RNA polymerase in avian and mammalian cells by a recombinant fowlpox virus. *J. Gen. Virol.*, **77**, 963–967.
11. Antin,P.B. and Ordahl,C.P. (1991) Isolation and characterization of an avian myogenic cell line. *Dev. Biol.*, **143**, 111–121.
12. Senne,D. (1989) Virus propagation in embryonating eggs. In Purchase,H.H., Arp,L.H., Domermuth,C.H. and Pearson,J.E. (eds), *A Laboratory Manual for the Isolation and Identification of Avian Pathogens*, 3rd edn. American Association of Avian Pathologists, Kendall, IA, pp. 176–181

13. Boot,H.J., ter Huurne,A.A.H.M., Vastenhouw,S.A., Kant,A., Peeters,B.P.H. and Gielkens,A.L.J. (2001) Rescue of infectious bursal disease virus from mosaic full-length clones composed of serotype I and II cDNA. *Arch. Virol.*, **146**, 1991–2007.
14. Boot,H.J., ter Huurne,A.A., Peeters,B.P. and Gielkens,A.L. (1999) Efficient rescue of infectious bursal disease virus from cloned cDNA: evidence for involvement of the 3′-terminal sequence in genome replication. *Virology*, **265**, 330–341.
15. Zuker,M. (1989) On finding all suboptimal foldings of an RNA molecule. *Science*, **244**, 48–52.
16. Dobos,P. (1995) The molecular biology of infectious pancreatic necrosis virus (IPNV). *Annu. Rev. Fish Dis.*, **5**, 25–54.
17. Pilipenko,E.V., Maslova,S.V., Sinyakov,A.N. and Agol,V.I. (1992) Towards identification of *cis*-acting elements involved in the replication of enterovirus and rhinovirus RNAs: a proposal for the existence of tRNA-like terminal structures. *Nucleic Acids Res.*, **20**, 1739–1745.
18. Yu,W. and Leibowitz,J.L. (1995) A conserved motif at the 3′ end of mouse hepatitis virus genomic RNA required for host protein binding and viral RNA replication. *Virology*, **214**, 128–138.
19. Friebe,P. and Bartenschlager,R. (2002) Genetic analysis of sequences in the 3′ nontranslated region of hepatitis C virus that are important for RNA replication. *J. Virol.*, **76**, 5326–5338.
20. Berkhout,B., Klaver,B. and Das,A.T. (1995) A conserved hairpin structure predicted for the poly(A) signal of human and simian immunodeficiency viruses. *Virology*, **207**, 276–281.
21. Yu,H., Grassmann,C.W. and Behrens,S.E. (1999) Sequence and structural elements at the 3′ terminus of bovine viral diarrhea virus genomic RNA: functional role during RNA replication. *J. Virol.*, **73**, 3638–3648.
22. vanRossum,C.M., Reusken,C.B., Brederode,F.T. and Bol,J.F. (1997) The 3′ untranslated region of alfalfa mosaic virus RNA3 contains a core promoter for minus-strand RNA synthesis and an enhancer element. *J. Gen. Virol.*, **78**, 3045–3049.
23. Reusken,C.B., Neeleman,L. and Bol,J.F. (1994) The 3′-untranslated region of alfalfa mosaic virus RNA 3 contains at least two independent binding sites for viral coat protein. *Nucleic Acids Res.*, **22**, 1346–1353.
24. Ford,L.P. and Wilusz,J. (1999) 3′-Terminal RNA structures and poly(U) tracts inhibit initiation by a 3′→5′ exonuclease *in vitro*. *Nucleic Acids Res.*, **27**, 1159–1167.
25. Huang,P. and Lai,M.M. (2001) Heterogeneous nuclear ribonucleoprotein a1 binds to the 3′-untranslated region and mediates potential 5′–3′-end cross talks of mouse hepatitis virus RNA. *J. Virol.*, **75**, 5009–5017.
26. Fujimura,T., Esteban,R., Esteban,L.M. and Wickner,R.B. (1990) Portable encapsidation signal of the L-A double-stranded RNA virus of *S.cerevisiae*. *Cell*, **62**, 819–828.
27. Tacken,M.G.J., Peeters,B.P.H., Thomas,A.A.M., Rottier,P.J.M. and Boot,H.J. (2002) Infectious bursal disease virus capsid protein VP3 interacts both with VP1, the RNA-dependent RNA polymerase and with viral double-stranded RNA. *J. Virol.*, **76**, 11301–11311.
28. Etchison,D., Milburn,S.C., Edery,I., Sonenberg,N. and Hershey,J.W. (1982) Inhibition of HeLa cell protein synthesis following poliovirus infection correlates with the proteolysis of a 220,000-dalton polypeptide associated with eucaryotic initiation factor 3 and a cap binding protein complex. *J. Biol. Chem.*, **257**, 14806–14810.
29. Piron,M., Vende,P., Cohen,J. and Poncet,D. (1998) Rotavirus RNA-binding protein NSP3 interacts with eIF4GI and evicts the poly(A) binding protein from eIF4F. *EMBO J.*, **17**, 5811–5821.
30. Chappell,S.A., Edelman,G.M. and Mauro,V.P. (2000) A 9-nt segment of a cellular mRNA can function as an internal ribosome entry site (IRES) and when present in linked multiple copies greatly enhances IRES activity. *Proc. Natl Acad. Sci. USA*, **97**, 1536–1541.
31. Mundt,E. and Muller,H. (1995) Complete nucleotide sequences of 5′- and 3′-noncoding regions of both genome segments of different strains of infectious bursal disease virus. *Virology*, **209**, 10–18.
32. Yao,K. and Vakharia,V.N. (1998) Generation of infectious pancreatic necrosis virus from cloned cDNA. *J. Virol.*, **72**, 8913–8920.